# Negative refraction index in the magnetic semiconductor $In_{2-x}Cr_xO_3$: Theoretical analysis

Adil-Gerai Kussow[1] and Alkim Akyurtlu[2]
[1]*Department of Physics, University of Massachusetts, Lowell, Massachusetts 01854, USA*
[2]*Electrical and Computer Engineering Department, University of Massachusetts, Lowell, Massachusetts 01854, USA*
(Received 2 March 2008; revised manuscript received 18 October 2008; published 12 November 2008)

Based on theoretical arguments, we have found that *homogeneous* indium oxide is a negative refractive index material if doped with Cr. In accordance with calculations, this magnetic semiconductor or $In_{2-x}Cr_xO_3$ in its polycrystalline form should possess a fully *isotropic* strongly pronounced negative refractive index at ~10.48 THz. The effect is due to the coexistence of the spin-wave mode with the plasmonic mode, and both modes are activated by the electromagnetic field of the light with simultaneous permittivity and permeability responses within the frequency band close to the ferromagnetic resonance. The analytical and numerical calculations of the frequency-dependent refractive index, $n(\omega)$, were conducted in the framework of the macroscopic theory of ferromagnets, the modified band theory, and the conduction electrons-mediated exchange integral formalism.

DOI: 10.1103/PhysRevB.78.205202 PACS number(s): 78.20.Bh, 75.50.Pp, 73.20.Mf

## I. INTRODUCTION

During the last several years, there has been tremendous interest in optical systems which possess a negative index of refraction. The existence of these systems, based on the analysis of Maxwell equations for the propagating electromagnetic (e.m.) wave, was predicted a long time ago in the papers of Mandel'shtam,[1] Lamb,[2] Shuster,[3] and Veselago.[4] In an idealized situation, if one neglects losses in both electric and magnetic subsystems, the permittivity, $\varepsilon$, and the permeability, $\mu$, are scalars rather than complex numbers. Such a medium with negative refractive index, $n<0$, is characterized by both negative permittivity, $\varepsilon<0$, and negative permeability, $\mu<0$, within some frequency range. This Veselago's condition to obtain negative refractive index was later generalized to take into account the losses or the complex nature of $\varepsilon=\varepsilon_1+i\varepsilon_2$, $\mu=\mu_1+i\mu_2$, and $n=n_1+in_2$.[5] In the calculation of complex refractive index, $n=\pm\sqrt{\varepsilon\mu}$, the sign in front of the radical is defined by the condition of passive media, $\mathrm{Im}(n)>0$,[6] and the negative refractive index corresponds to $\mathrm{Re}(n)<0$.

The so-called negative refraction medium demonstrates the optical properties or propagation characteristics, which are dramatically different from those in a medium with positive refractive index. Since, in this kind of an optical material, the Poynting vector and the phase velocity have opposite directions, it should reveal reversal of both the Doppler shift and Cherenkov radiation.[4] Moreover, due to the anomalous refraction, this material could be used to make, in principle, the perfect lens (or superlens) with the resolution beyond the standard optical limit.[7,8]

The theoretical and experimental researches on negative index metamaterials (NIMs) began in the microwave frequency range,[8] followed by the terahertz,[9] and finally, during last several years, has moved into the infrared[10,11] and optical region.[12–19] A great deal of difficulty in the study of NIMs originates from the fact that such optical systems are not natural substances. Natural materials with negative real part of the permittivity, $\varepsilon_1<0$, in some frequency range are not a rarity (e.g., metals, semiconductors, and gaseous plasma), but the substances with negative real part of permeability, $\mu_1<0$, which coexists with $\varepsilon_1<0$ is difficult to find. The examples of the materials with $\mu_1<0$ are ferrites, but then $\varepsilon_1>0$.[4] This situation is especially pronounced in the optical regime where the projection of spins onto the high-frequency, $\omega$, magnetic field is actually zero due to the low frequency, $\omega_p$, of spin precession when compared with the frequency of the e.m. wave (i.e., $\omega_p/\omega\leq 1\times 10^{-7}$). Hence, as follows from theoretical predictions,[20] any optical substance turns out to be principally nonmagnetic in the optical frequency range ($\mu=1$). Nevertheless, more recently, several authors have argued that due to the alternative quantum coherence mechanisms, atomic vapors (e.g., Rb) can possess a negative refractive index at optical range.[21–23]

The difficulty of finding natural media with negative refractive index has led to the creation of artificial substances possessing this effect. In these materials, complex $\varepsilon$, $\mu$, and $n$ are treated as effective parameters, $\varepsilon_{\mathrm{eff}}$, $\mu_{\mathrm{eff}}$, and $n_{\mathrm{eff}}$, respectively. We should emphasize that these parameters are obtained from the analytical and computational solutions to Maxwell's equations which describe the scattering of an e.m. wave in a principally inhomogeneous medium. In these inhomogeneous NIMs, multilayered structures,[13] plane dot structures,[15] quasiplane-arranged inclusion structures,[14] or the fishnet structure[18] were utilized at optical (infrared) range. For the 1–100 THz frequency range, the isotropic NIM design based on a fully symmetric multigap single-ring split-ring resonator (SRR) and crossing continuous wires was suggested in Ref 19. However, all of these designs are inhomogeneous, and a homogeneous medium compared to these designs would obviously not contain any inhomogeneity-driven losses and would be much easier to fabricate.

In this paper, we report a homogeneous optical negative refractive index material based on magnetic semiconductors (MS).[24] The specific magnetic semiconductor is the recently discovered Cr-doped indium oxide (IO).[25,26] The main idea of the magnon-plasmon interference mechanism which leads to the negative refractive index is the following. We achieve the negative refractive index effect by simply utilizing the well-known fact that in MS, the superposition of charge-density waves (plasmons) and spin-density waves (magnons)

 

is possible.[24] Consequently, we explore the opportunity by adjusting the appropriate parameters, such as the doping level, $x$, to adjust the plasmon resonance frequency to a value ($\omega_p \approx 10.8$ THz) larger than the limiting spin-wave resonance frequency of the ferromagnetic MS, $\Omega_S \approx 10.48$ THz, while remaining in the frequency region, in which the plasmon losses are minimized. We will show analytically, based on the theory of ferromagnetics,[27] that in polycrystalline MS, the appropriate permeability tensor, $\mu_{lk}(\omega)$, is reduced to a Drude-type scalar permeability function, $\mu(\omega)$. This permeability function describes the nonzero response, $\mu(\omega) \neq 1$, in the vicinity of the spin-wave resonance frequency, $\omega \approx \Omega_s$. This magnetic response is accompanied by the electric response, $\varepsilon(\omega)$, due to the plasmons, and the combination of both responses generates a negative index of refraction within some bands. The width of this band, $\Delta\omega$, also depends on the losses in the plasmonic and spin-wave subsystems, as we will show below.

The closest approach to our design to achieve a negative refractive index within a homogeneous material was recently reported in Ref. 28. It was shown experimentally that ferromagnetic metal manganite $La_{2/3}Ca_{1/3}MnO_3$ reveals a negative refractive index close to the frequency of the ferromagnetic resonance at ~150 GHz. The effect is based on the described above interplay between $\varepsilon(\omega)$ and $\mu(\omega)$ in the vicinity of the ferromagnetic resonance in such a way that the criteria of the negative refraction[5] are satisfied with $\mathrm{Re}(n) < 0$.

Our magnetic semiconductor IO doped with Cr possesses negative refraction at a much higher-frequency level ~10 THz compared to 150 GHz (Ref. 28) due to the *indirect* strong spin-spin ferromagnetic coupling which provides high limiting spin-wave (resonance) frequency, $\Omega_s \approx 10.48$ THz. Moreover, within the negative refraction band, our level of losses, $\xi = |\mathrm{Re}(n)/\mathrm{Im}(n)| \sim 0.4$, is much smaller than losses, $\xi \geq 1$, reported in Ref. 28. Also, our polycrystalline magnetic semiconductor $In_{2-x}Cr_xO_3$ reveals a fully isotropic effect if compared with highly anisotropic single-crystal manganite $La_{2/3}Ca_{1/3}MnO_3$.

Spin waves (magnons) were also utilized in the terahertz range of a hypothetical NIM in Ref. 29. However, this metamaterial is both inhomogeneous and highly anisotropic. In this situation, the suggested metamaterial consists of alternating layers of nonmagnetic semiconductor and nonconductive antiferromagnetic material. An attempt to reach a negative refractive index by using the amphoteric refraction conditions was developed in Ref. 30. Also, a similar approach based on the nonmagnetic semiconductors $In_{0.53}Ga_{0.47}As$ and $Al_{0.48}In_{0.52}As$ was reported recently in Ref. 31. As was explained in Ref. 32, both Refs. 30 and 31 actually do not involve the negative refractive index effect but rather illustrate the phenomenon of counterposition.[32]

The plan of the paper is as follows. Our main objective is to validate the negative refractive index effect in the proposed Cr-doped indium oxide. Since we need the analytical expressions for the permeability function, $\mu(\omega)$, for the problem of the polycrystalline sample, we will derive it first. The calculation of this so-called "orientational" permeability is conducted in the framework of both the macroscopic theory of ferromagnets and the classical scheme for the homogenization of $\mu(\omega)$ in polycrystals.[33,34] Second, we will calculate the limiting (resonance) spin-wave frequency, $\Omega_s$, which enters the expression for permeability function, $\mu(\omega)$, from the conduction electrons-mediated exchange integral formalism.[35] Next, based on the modified band theory,[36] we will calculate the plasmon frequency, $\omega_p$, which defines the Drude permittivity function, $\varepsilon(\omega)$, in MS, and which depends on the doping and the oxygen deficiency levels in Cr-doped indium oxide.[26] Finally, we will conduct parametric studies to reach a desirable negative refractive index and study the influence of the parameters of the plasmons and magnons on the effect.

## II. PERMEABILITY FUNCTION FOR POLYCRYSTALLINE FERROMAGNET

Our material of choice, the magnetic semiconductor, $In_{2-x}Cr_xO_3$, in its single-crystal form, possesses high-temperature ferromagnetism with a Curie temperature, $T_C > 300$ K.[26] The appropriate equilibrium magnetization, $M_0 \approx 3\mu_B N_{\mathrm{Cr}}$, where $N_{\mathrm{Cr}} = 1.6 \times 10^{22} (1/\mathrm{cm}^3)$, corresponds to the total moment, $J = 3/2$, of the randomly distributed $Cr^{3+}$ ions in $In_{2-x}Cr_xO_3$, with a density $N_{\mathrm{Cr}} \sim (0.1-1.6) \times 10^{22} (1/\mathrm{cm}^3)$, depends on the doping level $x < 1.0$. In our situation, $M_0$ is within the limits ~(100–300) $\mathrm{G}^{-1}$ depending on the values for $N_{\mathrm{Cr}}$. This theoretical value, $J = 3/2$, is in agreement with experimental results ($J \sim 1.8$) reported in Ref. 26, and the small difference $\Delta J/J \approx 0.15$, as we believe, is due to the background ferromagnetism of the undoped IO.

The single-crystal susceptibility tensor, $\chi_{l,j}(\omega)$, and hence, a permeability tensor, $\mu_{lj}(\omega) = 1 + 4\pi\chi_{l,j}(\omega)$, of a single-crystal ferromagnet is anisotropic.[27] In order to reduce the permeability tensor, $\mu_{l,j}(\omega)$, to permeability function, $\mu(\omega)$, we will consider a polycrystalline magnetic semiconductor, $In_{2-x}Cr_xO_3$.

Our calculations are based on the macroscopic theory of spin waves in single-crystal ferromagnets described in the most general form by Akhiezer *et al.*[27] In accordance with this formalism, the oscillations in the magnetization, $\vec{M}(\vec{r},t)$, of a single-crystal ferromagnet around the equilibrium value, $\vec{M}_0$, in the Fourier representation are expressed as

$$m_l(\vec{k},\omega) = \chi_{lj}(\vec{k},\omega) h_j(\vec{k},\omega), \tag{1}$$

where $h_l(\vec{k},\omega)$ and $m_l(\vec{k},\omega)$ are the $l$th Fourier components of the external frequency-dependent magnetic field and its response, appropriately, and $\chi_{l,j}(\vec{k},\omega)$ is the magnetic-susceptibility tensor,

$$\chi_{lj}(\vec{k},\omega) = \begin{pmatrix} \chi_{xx} & \chi_{xy} & 0 \\ \chi_{yx} & \chi_{yy} & 0 \\ 0 & 0 & 0 \end{pmatrix}, \tag{2}$$

$$\chi_{xx} = \frac{(g\mu_B M_0/\hbar)\Omega_1}{\Omega_1\Omega_2 - \omega^2}, \quad \chi_{yy} = \frac{(g\mu_B M_0/\hbar)\Omega_2}{\Omega_1\Omega_2 - \omega^2}, \tag{3}$$

$$\chi_{xy} = -\chi_{yx} = \frac{i\omega(g\mu_B M_0/\hbar)}{\Omega_1\Omega_2 - \omega^2},$$

$$\Omega_1 = (g\mu_B M_0/\hbar)\left(\alpha_{lj}k_l k_j + \frac{\vec{M}_0 \cdot \vec{H}_0^{(l)}}{M_0^2} + \beta\cos^2\psi\right),$$

$$\Omega_2 = (g\mu_B M_0/\hbar)\left(\alpha_{lj}k_l k_j + \frac{\vec{M}_0 \cdot \vec{H}_0^{(l)}}{M_0^2} + \beta\cos 2\psi\right). \quad (4)$$

Here, $\psi$ is the angle between the anisotropy axis, $\vec{n}$, and the vector, $\vec{M}_0$; the $z$ axis lies along $\vec{M}_0$ and the $x$ axis lies in the plane containing the vectors $\vec{n}$ and $\vec{M}_0$. $\beta$ is the magnetic anisotropy constant, $\mu_B$ is the Bohr magneton, $\alpha_{lj}$ is the tensor which describes the dispersion, $g$ is the spectroscopic splitting factor, and $\vec{H}_0^{(l)}$ is the internal magnetic field. The internal magnetic field, $\vec{H}_0^{(l)}$, depends on the external (applied) magnetic field $\vec{H}_0^{(e)}$ and the demagnetization tensor $\hat{N}$ as

$$\vec{H}_0^{(l)} = \vec{H}_0^{(e)} - 4\pi\hat{N}\cdot\vec{M}_0. \quad (5)$$

There are useful simplifications for the ferromagnet with cubic symmetry[27] ($In_{2-x}Cr_xO_3$ crystallizes with a bixbyite $C$-type cubic sesquioxide crystal structure). In these crystals, in the long-wave approximation, $\vec{k}=0$, $\vec{M}_0 \| \vec{H}_0^{(l)}$, and the tensor $\chi_{lj}(\omega)$ become symmetric in $x$ and $y$ directions;

$$\chi_{xx}(\omega) = \chi_{yy}(\omega), \quad \Omega_1 = \Omega_2 = \Omega_s,$$

$$\Omega_s = \left(g\frac{\mu_B}{\hbar}\right)(H_0^{(e)} - 4\pi\vec{N}\cdot\vec{M}_0) + g\left(\frac{\mu_B}{\hbar}\right)M_0\alpha\beta. \quad (6)$$

Here, $\alpha=2$ if the magnetization axis lies along the edge of the cube and $\alpha=4/3$ if it lies along the space diagonal of the cube. It should be mentioned that even in this situation, the tensor, $\chi_{lj}(\omega)$, although symmetric, is still anisotropic.

Expression (2) describes the magnetic-susceptibility tensor $\chi_{l,j}(\vec{k},\omega)$ of the low-frequency branch ($\omega \leq 1$ THz) of the collective spin-wave (magnon) excitations. As follows from Eq. (6), the resonance frequency, $\Omega_s$, increases with the doping density $N_{Cr}$ due to the magnetic dipole moment $M_0 \approx 3\mu_B N_{Cr}$. On other hand, the *optical high-frequency branch* $\omega \geq 1$ THz of the magnetic excitations corresponds to the motion of the individual spin in the local crystal magnetic field.[27] In this situation, the appropriate magnetic-susceptibility tensor due to the symmetry is still expressed by Eq. (2) with the Lorentzian components given by Eq. (3) but with modified resonance frequency $\Omega_s$.[27] Since $\Omega_s$ describes the local indirect interaction between the magnetic ion and the conduction electrons, rather than the direct interactions between magnetic ions, the limiting resonance frequency on the boundary of the Brillouin zone should not depend on the doping density, $N_{Cr}$ (III below). Indeed, this result was demonstrated by Liu[35] from the conduction electrons-mediated exchange integral formalism. Still, both the magnetic oscillation strength $f \sim M_0 \sim N_{Cr}$ [or the numerator of expression (3)] and, consequently, the magnetic permeability $\mu$ depends on $N_{Cr}$.

In our calculations we are interested in the high-frequency spin-wave problem within the (1–100) THz regime rather than in the low-frequency regime. As the following calculations demonstrated below, the limiting high-frequency (resonance), $\Omega_s \approx 10.48$ THz. In this frequency range, IO possesses the refractive index $n \approx 2$,[37,38] and the appropriate wavelength in the material is $\lambda \sim 15$ $\mu$m. This wavelength should be compared with the average typical size, $D$, of the polycrystal grain to find out if the homogenization of the permeability function, $\mu$, is possible.

To estimate $D$, one should consider the parameters of the typical low-angle grain boundary. The low-angle grain boundary is characterized by Burgers vector, $b \sim r_0 \sim 1 \times 10^{-8}$ (cm), of the edge dislocations which constitute the boundary[39,40] and which are separated an average distance, $L \gg b$. Due to the low-angle misorientation of the lattices, two adjacent grains produce almost identical permeability responses. Moreover, the contribution to the permeability from the normally nonmagnetic boundary is small due to the small thickness, $b$, of the boundary when compared with the size of the grain, $D$.[33] The misorientation low angle, $\theta \approx \frac{b}{L} \ll 1$, between adjacent grains is due to two neighboring edge dislocations on the boundary, and $D$ can be estimated as $D \approx L^2/b$. For the typical dislocation parameters, $b \approx 1 \times 10^{-8}$ (cm) and $L \sim (10-30)b$, the appropriate value for $D$ is $\sim 1$ $\mu$m, which is much smaller than $\lambda \sim 15$ $\mu$m. Hence, one may conclude that the homogenization of $\mu$ is possible, and one can employ the standard procedure for calculation of the effective or the so-called "rotational" permeability, $\mu_e$, of the polycrystal.[33] The aforementioned fact that the permeability changes smoothly between adjacent grains also supports the homogenization procedure due to small wave scattering by boundaries. In accordance with the homogenization approaches,[33,34] the macroscopic behavior of $\mu$ is isotropic for the randomly oriented grains in the polycrystal, and $\mu$ is reduced to an effective scalar value, $\mu_e$;

$$\mu_e = \frac{\mu_r D}{\mu_r \delta + D} \approx \mu_r, \quad (7)$$

where $\delta \sim b \ll D$ is the small thickness of the grain boundary and $\mu_r = 1 + 4\pi\bar{\chi}_{lj}$ is the rotational permeability[33] given by averaging the susceptibilities, $\chi_{lj}(\omega)$, of the differently oriented grains over their randomly distributed orientations,

$$\bar{\chi}_{lj}(\omega) = \int\int\int d\alpha d\beta d\gamma \sum_{p,q=1}^{3} \chi_{p,q}(\omega)\{A^{-1}\}_{pl}\{A^{-1}\}_{qk}. \quad (8)$$

Here, $\hat{A}(\alpha,\beta,\gamma)$ is the rotational matrix which depends on the Euler angles $\{\alpha,\beta,\gamma\}$. The appropriate calculation of the integral in Eq. (8) reduces the tensor $\chi_{lj}(\omega)$ given by Eq. (2) to the scalar susceptibility function $\chi(\omega) = (\frac{2}{3})\frac{(g\mu_B/\hbar)M_0\Omega_s}{\Omega_s^2 - \omega^2}$, which generates the following Drude-type rotational magnetic permeability function:

$$\mu(\omega) = 1 + \frac{2}{3}\frac{(4\pi g\mu_B/\hbar)M_0\Omega_s}{\Omega_s^2 - \omega^2}. \quad (9)$$

The permeability function, since complex, should include the losses, $\Gamma$, and the imaginary part of $\mu(\omega)$ can be recovered from the real part of $\mu(\omega)$ [Eq. (9)] by the standard Kramers-Kronig transformation. The appropriate analytical Kramers-Kronig calculation, with high accuracy $[1-(\Gamma/\Omega_S)^2 \sim 1$ and

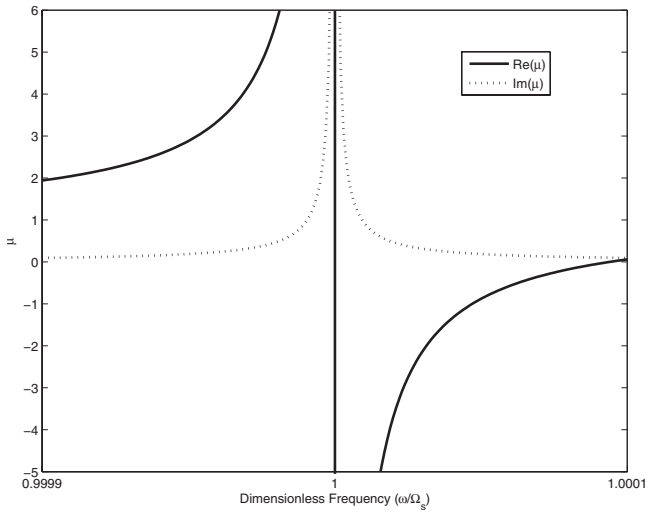


FIG. 1. The real, Re$[\mu(\tilde{\omega})]$, and the imaginary, Im$[\mu(\tilde{\omega})]$, parts of the permeability function from Eq. (10) in dimensionless units, $\tilde{\omega}=\omega/\Omega_s$, with losses, $\Gamma/\Omega_s=0.1$, and $N_{\mathrm{Cr}}=1.6\times10^{22}$ cm$^{-3}$ which corresponds to $x=1.0$

$\Gamma/\Omega_S \ll 1$], provides the following expression for the complex $\mu(\omega)$:

$$\mu(\omega)=1+\frac{(8\pi g\mu_B M_0\Omega_s/3\hbar)}{\Omega_s^2-\omega^2}+\frac{i\omega\Gamma(8\pi g\mu_B M_0\Omega_s/3\hbar)}{|\Omega_s^2-\omega^2|\Omega_s^2}. \tag{10}$$

The results of the numerical Kramers-Kronig calculations with an accuracy of ~95% were found to be close to the analytical expression (10) within the range of parameters of interest.

Alternatively, the reasonable approximation for $\mu(\omega)$ can be obtained from Eq. (9) by the formal substitution $\omega\rightarrow\omega+i\Gamma$ in the denominator. Since the Kramers-Kronig calculation is obviously more rigorous and is close to the numerical results, despite of the inherent singularity in Re$[\mu(\omega)]$ at the resonance, we will use Eq. (10) in the following analysis.

As follows from Eq. (10), near the resonance, $\omega\approx\Omega_s$, within the narrow window $\Delta\omega_\mu/\Omega_s\ll1$, there is a considerable magnetic response with both the positive, Re$[\mu(\omega)]>0$, and the negative, Re$[\mu(\omega)]<0$, real parts of the permeability, as illustrated in dimensionless units in Fig. 1.

Hence, for any polycrystalline ferromagnet with cubic symmetry, close to the ferromagnetic resonance, $\omega\approx\Omega_s$, the frequency window always exists with considerable magnetic response, $|\mu|\geq1$.

As we will show below, the permeability function from Eq. (10), combined with the Drude permittivity function, $\varepsilon(\omega)$, provides a refractive index,[5,6] $n(\omega)=\sqrt{\mu(\omega)\varepsilon(\omega)}$, with a negative real part Re$[n(\omega)]<0$ within some band, $\Delta\omega\sim\Delta\omega_\mu$, close to the ferromagnetic resonance frequency, $\Omega_s$.

### III. SPIN-WAVE (MAGNON) FREQUENCY

As follows from expression (10), the permeability function, $\mu(\omega)$, depends on the spin-wave (magnon) frequency, $\Omega_s$. Hence, $\Omega_s$ needs to be calculated or at least estimated with the highest possible accuracy. The spin-wave dispersion relation for crystals with cubic symmetry is isotropic in the $q$ space and is given by[27]

$$\omega(\vec{q})\approx\left(\frac{W_J}{\hbar}\right)\left[1-\cos\left(\frac{qr_0}{2}\right)\right], \tag{11}$$

with the wave vector $\vec{q}$, $0<q<\pi/r_0$ within the Brillouin zone, and $W_J$ as the exchange integral which depends on the details of the spin-spin interaction mechanisms. The limiting spin-wave frequency, $\omega_{\max}\approx W/\hbar$, on the boundary of the Brillouin zone ($q_{\max}=\pi/r_0$) corresponds to the exchange integral, $W_J$, which describes the interaction of an individual magnetic ion ($Cr^{3+}$) with the lattice. This limiting frequency, $\omega_{\max}=\Omega_s$, is associated with the resonance frequency, $\Omega_s$, from expressions (9) and (10) for the permeability. Hence, the limiting spin-wave (resonance) frequency, $\Omega_s=W_J/\hbar$, is defined by the exchange integral, $W_J$. In its turn, the exchange integral, $W_J$, critically depends on the specific mechanism of the ferromagnetism in Cr-doped IO. In accordance with the experimental data,[26] the strong ferromagnetic ordering of Cr-doped IO takes place even at a small doping level (i.e., $x\leq0.1$) and is unlikely to be due to the direct exchange mechanism because of the large separation of magnetic Cr ions. Hence, the indirect exchange mechanism due to the conduction electrons mediated exchange should be responsible for the ferromagnetism in Cr-doped IO. Consequently, our calculation of $\Omega_s=W_J/\hbar$ is based on the appropriate Liu theory of the indirect exchange developed in Ref. 35. In this theory, the exchange Coulomb interaction between magnetic shell electrons of the impurity (or ion) and the conduction electrons is derived analytically from first principles. The Liu model considers the magnetic ion ($Cr^{3+}$) with unfilled shell and noncompensated moment, $J=|L-S|$. Here, $L$ is the orbital moment and $S$ is the total spin of the shell calculated in accordance with the Hund rule. The magnetic ions are in a sea of conduction electrons, and each ion interacts with conduction electrons so the total interaction can be obtained by summing overall the conduction electrons and all the ions. The conduction electron belongs simultaneously to the whole crystal and to the $3d$ shell of the ion which is less than half filled. In accordance with both the Pauli principle and the Hund rule, there are three electrons in $3d$ outer magnetic shell with $m=2$, 1, and 0 projections of the orbital moment $l=2$ onto the fixed $z$ axis. Consequently, Liu's[35] exchange Hamiltonian, $H$, which describes the interaction of the magnetic ion with the sea of the conduction electrons, does not depend on either the density of magnetic ions ($N=N_{\mathrm{Cr}}$) nor the density of conduction electrons, $n_e$. The appropriate expression for Liu's[35] Coulomb exchange Hamiltonian, with the eigenvalue $H_0=W_J$, is given by

$$H=-2I(k,k')(g-1)\vec{s}\vec{J}, \tag{12}$$

where $s$ is the spin of the conduction electron and $k,k'$ are the wave vectors of the initial and the final state of the conduction electron, respectively. The exchange energy $I(k,k')$ is given by

$$I(k,k') = \frac{4\pi e^2}{(2l+1)} \int_{r1,} \int_{r2} R^*(r_j) R(r_{N+1}) u_0^*(r_{N+1}) u_0(r_j) j_0 \times (k' r_{N+1}) j_0(k r_j) \frac{(r_<)^l}{(r>)^{l+1}} r_{N+1}^2 r_j^2 dr_j dr_{N+1}, \quad (13)$$

with the spectroscopic splitting factor,

$$g = 1 + [J(J+1) + S(S+1) - L(L+1)]/2J(J+1). \quad (14)$$

Here, the wave function of the conduction electron, $\phi(\vec{r},s)$, assumes the Bloch form,

$$\phi(\vec{r},s) = u_k(\vec{r}) \exp(i\vec{k}\vec{r})\chi, \quad (15)$$

where $\chi$ is the Pauli spinor. The $r_j$ and $r_{N+1}$ are the coordinates of the electron in magnetic shell and in conduction band, respectively, $e$ is the charge of an electron, and $l$ is the orbital moment of the electron in magnetic shell of an ion. The function $R(r)$ is the $r$-dependent coordinate function of the Bohr atom and $j_0(kr) = \sin(kr)/kr$ is the Bessel function of zero order. The atomic configurations of the Cr atom and the $Cr^{3+}$ ions are appropriately $Cr: 1s^2 2s^2 2p^6 3s^2 3p^6 3d^5 4s^1$ and $Cr^{3+}: 1s^2 2s^2 2p^6 3s^2 3p^6 3d^3$, and the $Cr^{3+}$ ion magnetic shell parameters are $S=3/2$, $L=3$, and $J=3/2$. In accordance with first-principles calculations,[38,41] the conduction electron of the Bloch state, in IO, has an effective mass of $m_{\text{eff}} \approx 0.3 m_e$ ($m_e$ is the mass of an electron). Since the resonant Cr $d$ states do not hybridize with the $s$ states of indium and do not affect the dispersion of the conduction band,[41] the effective mass of $In_{2-x}Cr_xO_3$ should be similar to the one of pure IO. Also, we will make the standard assumption that the conduction electron is in $4s^1$ state and the mixture of the $p$ state is small. This assumption allows the estimation of the largest magnitude of the exchange integral since the mixture of non-$s$ states decreases the integral $I(k,k')$.[35]

The appropriate wave functions $R(r) = R_{n=3,l=2}(r)$ and $u_k(r) = u_o(r) = R_{n=4,l=0}(r)$ are given below;

$$R_{32}(r) = \left(\frac{2z}{3a_0}\right)^{3/2} \frac{1}{12\sqrt{5}} \exp\left[-\frac{1}{2}\left(\frac{2zr}{3a_0}\right)\right]\left(\frac{2zr}{3a_0}\right), \quad (16)$$

$$u_0(r) = R_{40}(r) = \left(\frac{z}{2a_{01}}\right)^{3/2} \left(4 - 6\rho + 2\rho^2 - \frac{1}{8}\rho^3\right) \exp\left(-\frac{1}{2}\rho\right),$$

$$\rho = \frac{zr}{2a_{01}}, \quad a = \frac{\hbar^2}{me^2}, \quad a_{01} = \frac{\hbar^2}{m_{\text{eff}} e^2}. \quad (17)$$

The calculation of the two-dimensional (2D) exchange integral [Eq. (13)] was performed by a Monte Carlo algorithm (VEGAS) described elsewhere[42] with an accuracy of ~0.001. The spin-wave frequency, $\Omega_s = W_J/\hbar = H/\hbar$, as calculated from the Hamiltonian [Eq. (12)], was found to be close to $\Omega_s = 10.48$ THz. Since the calculated ferromagnetic spin-wave coupling $\hbar\Omega_s \sim 1.8kT$ is approximately two times larger than the thermal energy $kT$ at room temperature, our result supports the experimentally verified Curie temperature in $In_{2-x}Cr_xO_3$ which is well above 300 K.[26] The substitution of the magnon (spin-wave) frequency, $\Omega_s$, into expression (10) generates the frequency-dependent permeability function, $\mu(\omega)$, of interest.

## IV. PERMITTIVITY FUNCTION

The plasmon frequency, $\omega_p$, enters the extended Drude expression[43] for the permittivity function of a semiconductor, $\varepsilon(\omega)$, with losses, $\gamma$, as follows:

$$\varepsilon(\omega) = \varepsilon_\infty \left(1 - \frac{\omega_p^2}{\omega^2 + i\gamma\omega}\right), \quad (18)$$

where $\varepsilon_\infty \approx 0.8$ (Ref. 38) is the permittivity at infinite frequency. In its turn, $\omega_p$, depends on the density, $n_c$, of the electric charges (electrons in our situation of Cr-doped IO[26]),

$$\omega_p = \sqrt{\frac{4\pi n_c e^2}{\varepsilon_\infty m_{\text{eff}}}}. \quad (19)$$

Hence, in order to find the permittivity function, $\varepsilon(\omega)$, one needs to calculate the density of the electrons in the conduction band, $n_c$. The density, $n_c$, depends on two factors: the doping level, $x$, or the density of Cr ions, $N_{\text{Cr}}$, and the density of the oxygen deficiency, $N_{\text{O}}$, at the fabrication stage.[25,44] In accordance with the experimental data,[25,44] the main source of free-electron carriers in IO is the nonstoichiometric oxygen deficiency. Still, in our calculation of $n_c$, we will also take into account the possible electron donation into $n_c$ from the Cr atoms. In the calculation of $n_c$ we will utilize the modified band-theory approach[36] where the input parameters are the density of an oxygen deficiency $N_{\text{O}}$ (which depends on the details of fabrication, such as oxygen pressure[44]) and the density $N_{\text{Cr}}$ of Cr ions.

In an attempt to increase the accuracy of the calculations of $n_c$, we utilize the modified band-theory model.[36] The modification to the standard band-theory calculation[36] comes from the mutual repulsion of electrons on donors' Bohr orbits which will effectively reduce the splitting of the donor level from the bottom of the conduction band. This qualitative result follows from the positive sign of $e$-$e$ repulsion energy when compared with negative sign of the splitting of donor level from the bottom of the conduction band in band-theory model.

We will consider the simple model when each ion ($Cr^{3+}$ or $O^{2+}$) is surrounded by six atoms of the same nature; so the distance between two neighbors, $l$, is a free parameter which can be calculated from the concentration $N_{\text{Cr,O}}$ of the ions in the matrix,

$$l = \frac{1}{(N_{\text{Cr,O}})^{1/3}}. \quad (20)$$

Since the wave functions of the nearest ions overlap, one can calculate the appropriate Coulomb energy correction given by $\Delta E_d = 3^* \Delta E_{e\text{-}e}$ due to the overlapping. As a result, the splitting energy, $E_{d\text{-corr}}$, of a donor is the sum of the standard band-theory result[24] $E_d$ plus the Coulomb correction $\Delta E_d$,

$$E_{d\text{-corr}} = E_d + 3^* \Delta E_{e\text{-}e} = -\left(\frac{Z}{n}\right)^2 \frac{m_{\text{eff}} e^4}{2\hbar^2 \varepsilon_0^2} + 3^* \Delta E_{e\text{-}e}, \quad (21)$$

with $\varepsilon_0 \approx 4.4$ as the static dielectric constant of IO,[37] $n$ is the Bohr orbit number, $Z$ is the charge of an ion, and the energy is measured from the bottom of the conduction band.

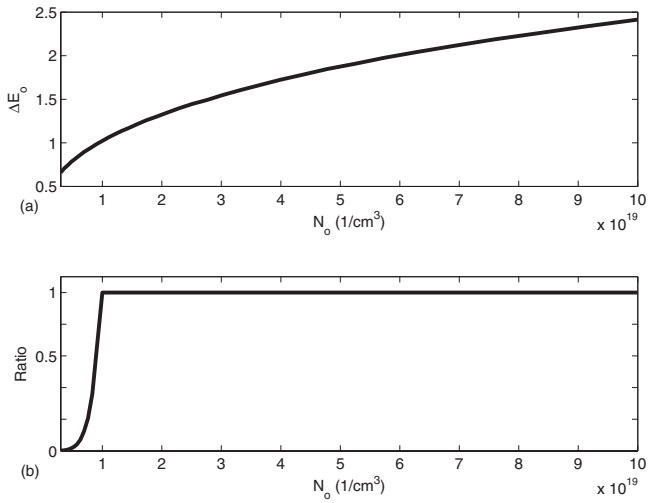


FIG. 2. Extended band-theory calculation of the donation rate $k_O$ of oxygen deficiency ions. (a) Coulombic repulsion energy $\Delta E_{e\text{-}e}$ for oxygen ions (eV). (b) Dimensionless donation ratio $k_O = n_c / N_O$ for oxygen ions.

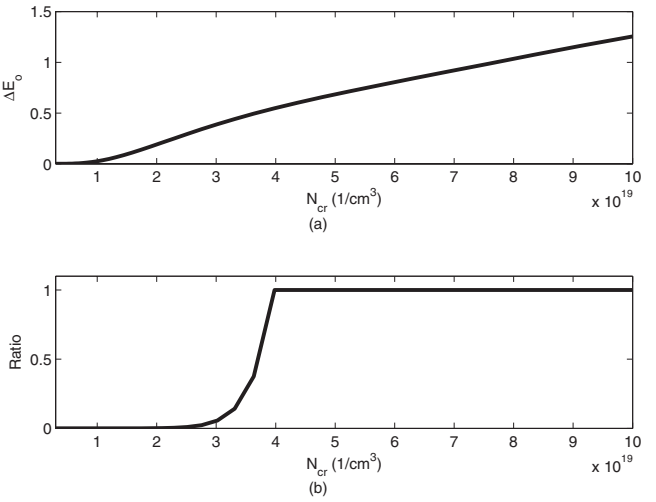


FIG. 3. Extended band-theory calculation of the donation rate $k_{Cr}$ for Cr ions. (a) Coulombic repulsion energy $\Delta E_{e\text{-}e}$ for Cr ions (eV). (b) Dimensionless donation ratio $k_{Cr} = n_c / N_{Cr}$ for Cr ions.

Since the second term is positive and the first term is negative, the Coulomb correction decreases the absolute value of splitting energy, pushing electrons from the donor level into the conduction band. Hence, the Coulombic term always increases the donation of the electrons into the conduction band. Consequently, we should substitute the expression for the density of the donated electrons into the conduction band from the standard band theory,[24]

$$n_c = \sqrt{\frac{N_{\mathrm{Cr,O}} N_{\mathrm{eff}}}{2}} \exp\left\{ - \frac{|E_d|}{2 k_B T} \right\}, \tag{22}$$

by the following expression with Coulomb energy correction,

$$n_c = \sqrt{\frac{N_{\mathrm{Cr,O}} N_{\mathrm{eff}}}{2}} \exp\left\{ - \frac{|E_{d\text{-corr}}|}{2 k_B T} \right\}, \tag{23}$$

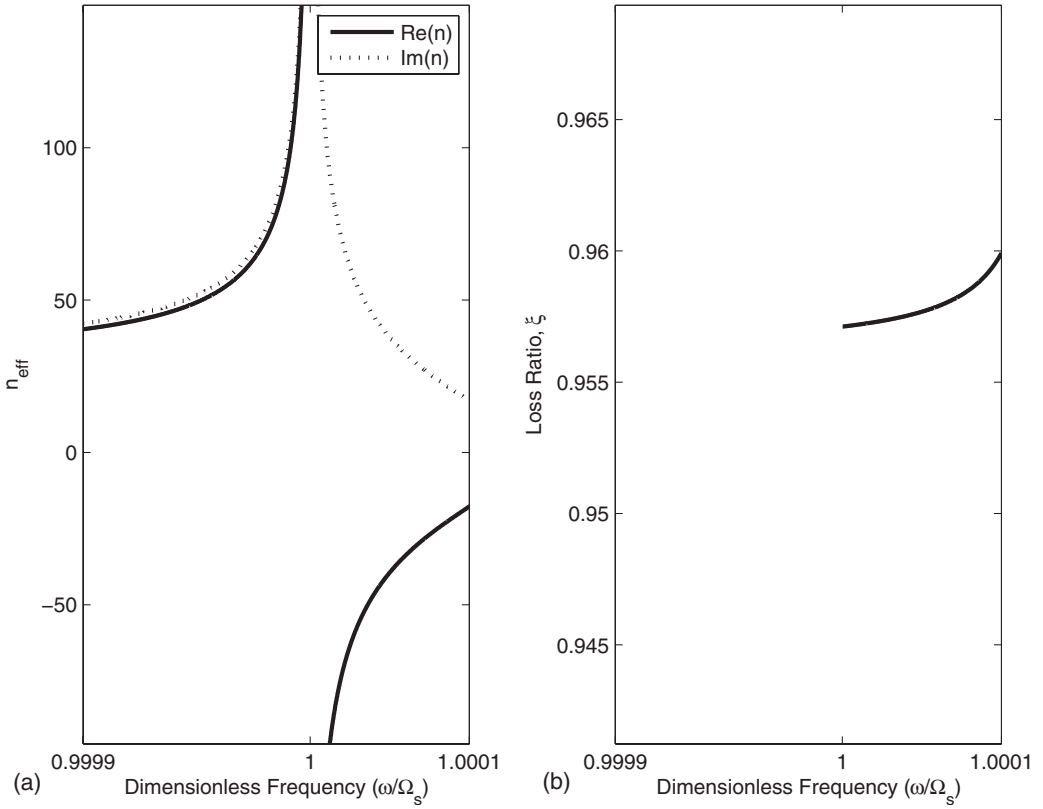


FIG. 4. (a) The index of refraction and (b) the loss ratio $\xi = \left| \frac{\mathrm{Im}(n)}{\mathrm{Re}(n)} \right|$ for heavily doped ($x = 1.0$) IO with $N_{Cr} = n_e = 1.6 \times 10^{22}$ (1/cm$^3$) and losses $\gamma / \omega \sim 0.1$ and $\Gamma / \Omega_s \approx 1 \times 10^{-3}$.

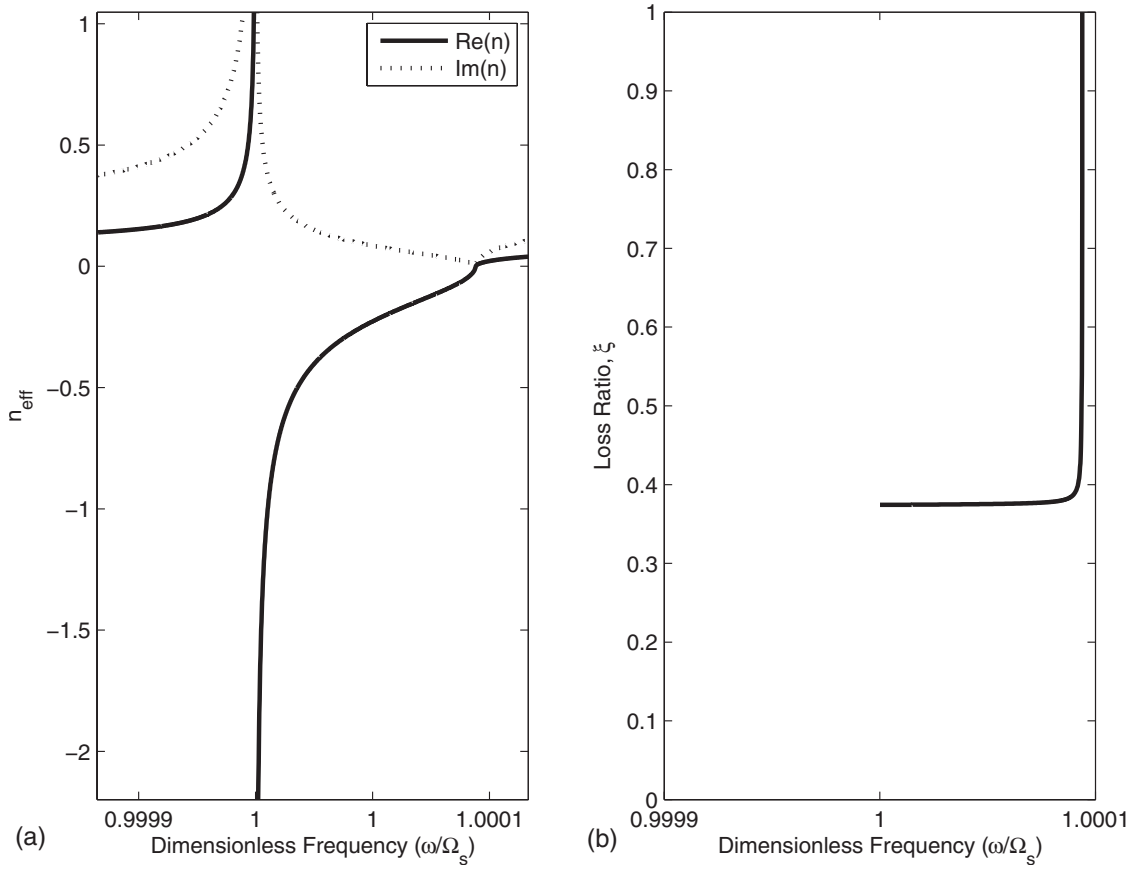


FIG. 5. (a) The index of refraction and (b) the loss ratio $\xi=\left|\frac{\mathrm{Im}(n)}{\mathrm{Re}(n)}\right|$ for heavily doped ($x=1.0$) of IO with Cr and acceptor: $N_{\mathrm{Cr}}=1.6\times10^{22}$ cm$^{-3}$, $n_e=3.5\times10^{17}$ cm$^{-3}$ and $\gamma/\omega\sim0.1$ for $\Gamma/\Omega_s\approx1\times10^{-3}$.

$$N_{\mathrm{eff}}=\frac{1}{4\pi^2}\left(\frac{2\pi m_{\mathrm{eff}}k_BT}{\hbar^2}\right)^{3/2}. \tag{24}$$

Since the magnitude of the $\Delta E_{e\text{-}e}$ correction increases with concentration of ions, this correction will unconditionally increase the donation rate when the distance between ions becomes smaller (or the concentration of ions, $N_{\mathrm{Cr,O}}$, becomes larger). Ultimately, Eq. (23) provides the full donation ($n_c/N_{\mathrm{Cr,O}}\sim1$) from the donor level into the conduction band if the densities, $N_{\mathrm{Cr,O}}\approx N_{\mathrm{Cr,O}}^{\mathrm{crit}}$, are large enough. This situation physically corresponds to the insulator-metal transition,[24] and we will calculate the $n_c$ and the threshold critical densities, $N_{\mathrm{Cr,O}}^{\mathrm{crit}}$. We should emphasize that the approximation of the band theory breaks down when $N_{\mathrm{Cr,O}}>N_{\mathrm{Cr,O}}^{\mathrm{crit}}$ (Ref. 36) and $n_c/N_{\mathrm{Cr,O}}\sim1$.

The overlapping integral, $\Delta E_{e\text{-}e}$, in Eq. (21) depends on the spins of two electrons located on nearest ions. The singlet and triplet states are possible, and these states will give varying results for $\Delta E_{e\text{-}e}$ with an accuracy of an exchange energy. Despite the fact that the exchange term is smaller than singlet or triplet energies, we wish to take this effect into account by the calculation of the energy $E_{e\text{-}e}$ averaged over both states,

$$\Delta E_{e\text{-}e}=\frac{1}{2}\int_{r_1}\int_{r_2}[\phi_S^*(r_1,r_2)\phi_S(r_1,r_2)+\phi_A^*(r_1,r_2)\phi_A(r_1,r_2)]\frac{e^2}{|r_1-r_2|}dr_1^3dr_2^3, \tag{25}$$

with the singlet ($S$) and triplet ($A$) wave functions of the standard form,

$$\phi_S(r_1,r_2)=\frac{1}{\sqrt{2}}\{\varphi_a(r_1)\varphi_b(r_2)+\varphi_a(r_2)\varphi_b(r_1)\},$$

$$\phi_A(r_1,r_2)=\frac{1}{\sqrt{2}}\{\varphi_a(r_1)\varphi_b(r_2)-\varphi_a(r_2)\varphi_b(r_1)\}. \tag{26}$$

The calculation of the six-dimensional (6D) exchange integral (25) was performed by the Monte Carlo VEGAS algorithm.[42] The calculated corrections to energy $\Delta E_{e\text{-}e}$ and the donation rates $n_c/N_{\mathrm{Cr,O}}$ as the functions of the density of ions $N_{\mathrm{Cr,O}}$ are shown in Figs. 2 and 3.

One can see from Figs. 2 and 3 that in both situations of Cr ions and oxygen deficiency ions, the corrections to the energy $\Delta E_{e\text{-}e}$ and the donation ratios $n_c/N_{\mathrm{O,Cr}}$ increase slowly with the density of ions until some threshold critical densities $N_{\mathrm{Cr,O}}^{\mathrm{crit}}$. The appropriate critical densities $N_{\mathrm{O}}^{\mathrm{crit}}\sim1\times10^{19}(1/\mathrm{cm}^3)$ and $N_{\mathrm{Cr}}^{\mathrm{crit}}\sim4.0\times10^{19}(1/\mathrm{cm}^3)$ correspond to

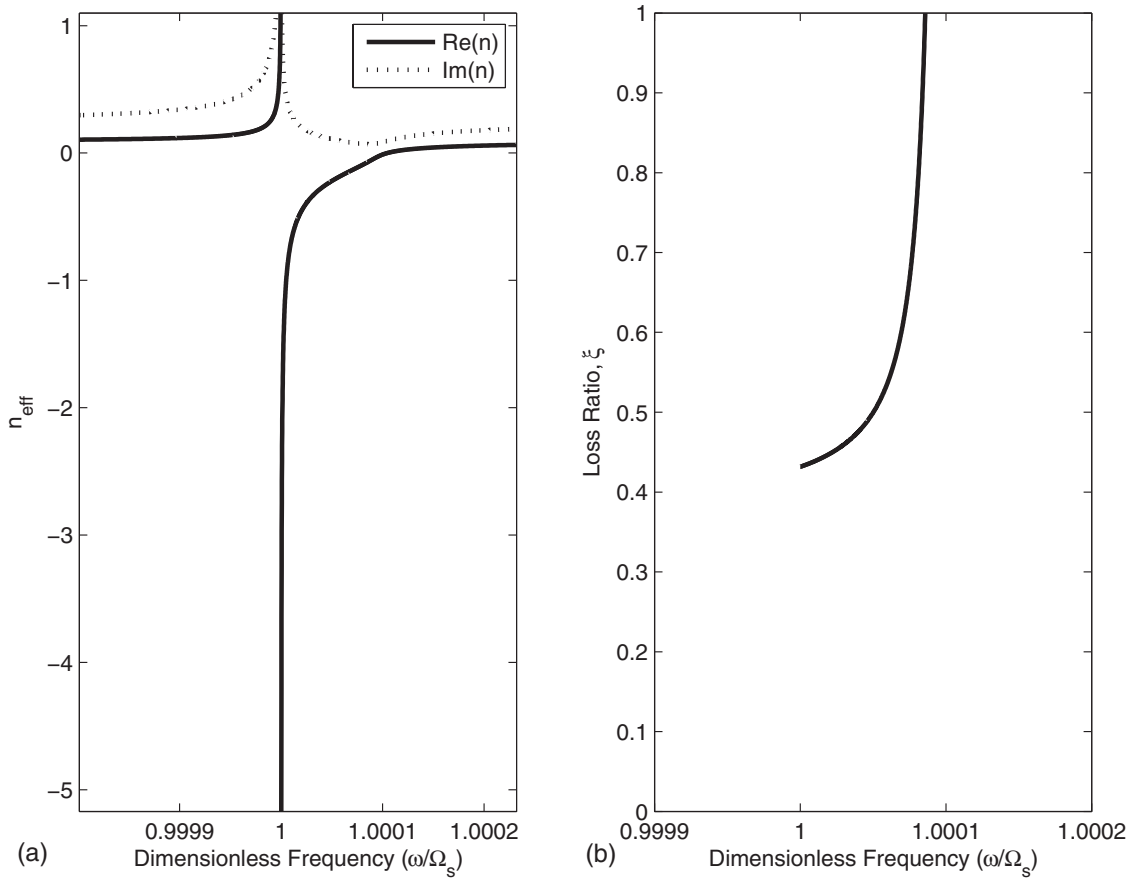


FIG. 6. (a) The index of refraction and (b) the loss ratio $\xi=\left|\frac{\mathrm{Im}(n)}{\mathrm{Re}(n)}\right|$ for heavily doped ($x=1.0$) of IO with Cr and acceptor: $N_{\mathrm{Cr}}=1.6\times10^{22}$ cm$^{-3}$, $n_e=3.5\times10^{17}$ cm$^{-3}$ and $\gamma/\omega\sim0.1$ for $\Gamma/\Omega_s\approx1\times10^{-1}$.

the total donation $n_c/N_{\mathrm{O,Cr}}\sim1.0$ or insulator-metal transition.[24] One should emphasize that the onset of the total donation happens at much smaller critical density of oxygen deficiency than the critical density of chromium ($N_{\mathrm{O}}^{\mathrm{crit}}/N_{\mathrm{Cr}}^{\mathrm{crit}}\sim0.25$). Hence, one can conclude that the oxygen deficiency donates the electrons into the conduction band much more effectively than the Cr ion. This result partially justifies the conclusions of experimental papers[26,44] that in undoped IO, the mechanism of donation is due to the oxygen deficiency. But we should add that in accordance with our calculations described above, Cr ions donate electrons as well although at higher densities. In other words, the total donation rate is the sum of two rates $k=k_{\mathrm{O}}+k_{\mathrm{Cr}}$, and even in an ideally fabricated Cr-doped IO, with no oxygen deficiencies (e.g., at high oxygen pressure on fabrication phase[44]), the conduction band still will be populated due to the donation from Cr ions.

Finally, the substitution of the calculated density of electrons in the conduction band, $n_c$, into the expression for the plasmon frequency, $\omega_p$, given by Eq. (19), and Eq. (19) into Eq. (18) determines the permittivity, $\varepsilon(\omega)$, as a function of densities of Cr ions, $N_{\mathrm{Cr}}$, and oxygen deficiency, $N_{\mathrm{O}}$. The densities $N_{\mathrm{Cr}}$ and $N_{\mathrm{O}}$ are input parameters for calculation of the permittivity function [Eqs. (18) and (19)], and they depend on the doping level, $x$, for Cr, $[N_{\mathrm{Cr}}=1.6\times10^{22}(1/\mathrm{cm}^3)]$, and the fabrication details for the oxygen deficiency (e.g., oxygen pressure). The density $n_e=N_{\mathrm{Cr}}$ also affects the magnetization $M_0\approx3\mu_B N_{\mathrm{Cr}}$ which enters expression (10) for the permeability function. In accordance with experimental data,[25,26] in Cr-doped IO, the typical total plasmon losses, which are due to the scattering of electrons by electrons, phonons, and defects can be estimated as $\gamma_0/\omega_p\sim0.1$.

## V. REFRACTIVE INDEX CALCULATIONS

Expressions (10), (18), and (19) are utilized to calculate the frequency-dependent refractive index, $n(\omega)$, for the specified level of doping, $x$ (or the density $N_{\mathrm{Cr}}=1.6\times10^{22}$ cm$^{-3}$ of Cr atoms). In this calculation, we will consider the situation when the oxygen deficiency is suppressed at the fabrication stage (e.g., high oxygen pressure[44]); so the only source of the conduction electrons is Cr ions ($n_e=N_{\mathrm{Cr}}$). Also, for the sake of simplicity, we have assumed a small driven external field $H_0^{(e)}\approx0$. In expression (10), which describes the permeability function, the equilibrium magnetization $M_0\approx3\mu_B N_{\mathrm{Cr}}$ is proportional to the product of nonsaturated total magnetic moment $M=3\mu_B$ of the Cr ion and the density of the Cr atoms. In expressions (18) and (19) for the permittivity function, the density of the electrons $n_c(N_{\mathrm{Cr}})$ in the conduction band depends on $N_{\mathrm{Cr}}$, and one should consider two different scenarios of donation, which correspond to insulatorlike or metal-like situations, appropriately.

As follows from our calculations described in Sec. VI, in the situation of heavy doping when the density of Cr atoms is

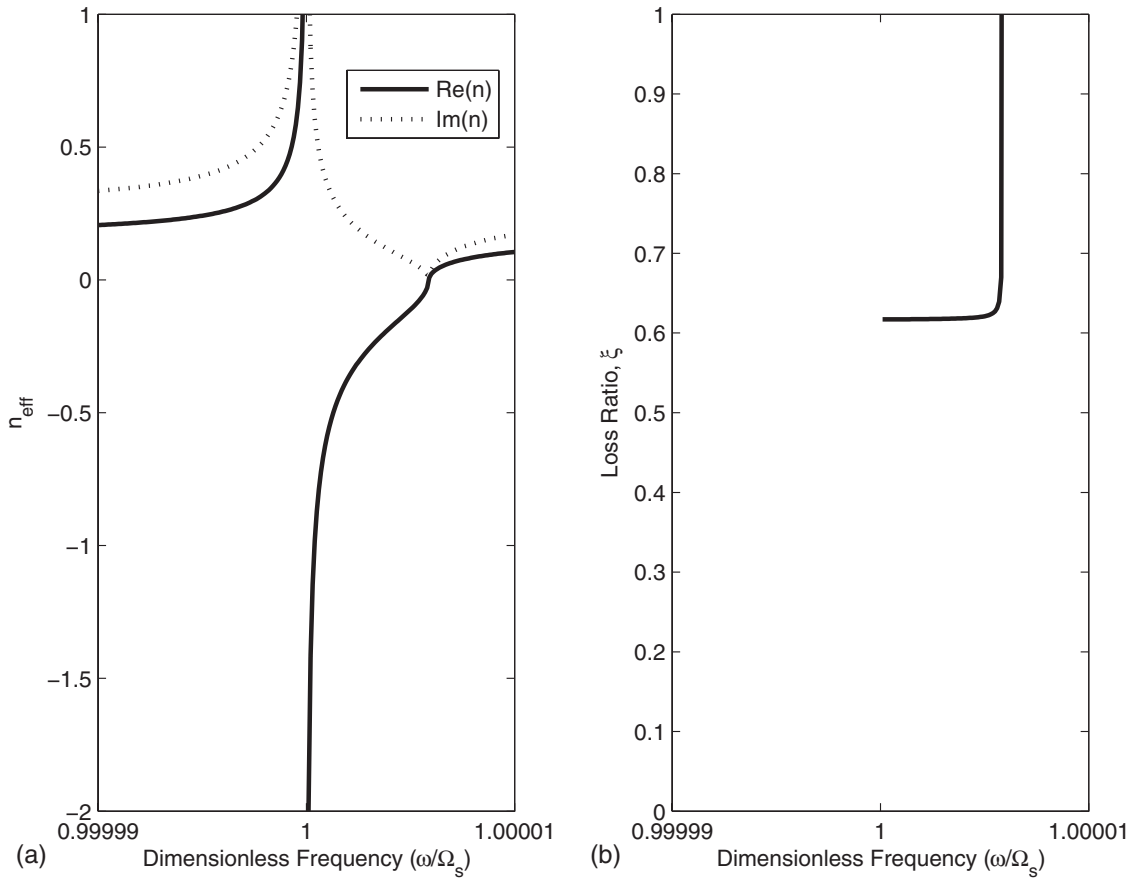


FIG. 7. (a) The index of refraction and (b) the loss ratio $\xi=|\frac{\mathrm{Im}(n)}{\mathrm{Re}(n)}|$ for moderate doping ($x=0.06$) of IO with Cr and acceptor: $N_{\mathrm{Cr}}=1.0\times10^{21}(1/\mathrm{cm}^3)$, $n_c=3.5\times10^{17}(1/\mathrm{cm}^3)$ and $\gamma/\omega_{\mathrm{p}}=0.1$ for $\Gamma/\Omega_s\approx1\times10^{-3}$.

larger than the threshold of the insulator-metal transition $N_{\mathrm{Cr}}\geq N_{\mathrm{Cr}}^{\mathrm{crit}}\sim4.0\times10^{19}(1/\mathrm{cm}^3)$ (metal-like), the Cr ions donate all electrons into the conduction band and $n_c(N_{\mathrm{Cr}})\approx N_{\mathrm{Cr}}$. In the situation of modest doping $N_{\mathrm{Cr}}<N_{\mathrm{Cr}}^{\mathrm{crit}}\sim4.0\times10^{19}(1/\mathrm{cm}^3)$ (insulatorlike), the donor Cr atoms donate electrons into the conduction band only partially $n_c<N_{\mathrm{Cr}}$.

Initially, calculations of the refractive index[5,6] for heavy doping, where $N_{\mathrm{Cr}}=n_e=1.6\times10^{22}(1/\mathrm{cm}^3)$, with doping level [$x=1.0(\sim20\%$ Cr)] were conducted. In this calculation, we have utilized experimentally verified levels of losses in the plasmonic subsystem, $\gamma/\omega\sim0.1$.[25,26] In accordance with both experimental and theoretical data,[45–48] depending on the specific ferromagnetic, the losses in the spin-wave system can change in a very broad range ($1\times10^{-5}<\Gamma/\Omega_s<1\times10^{-3}$), and they can be much larger ($\Gamma/\Omega_s\leq1\times10^{-1}$) on the boundary of the Brillouin zone at resonance[49,50] [examples are Co (Ref. 49) and Fe (Ref. 50)]. Since, for our specific material, the exact magnitude of losses is not known, we have considered different levels of losses, including the large losses, $\Gamma/\Omega_s\approx0.1$.

The result of the calculation with the moderate losses, $\Gamma/\Omega_s\approx1\times10^{-3}$, in the spin-wave subsystem is shown in Fig. 4, and one can see a strongly pronounced [$\mathrm{Re}(n)\sim-50$] negative refractive index band with a high loss ratio, $\xi=|\mathrm{Im}(n)/\mathrm{Re}(n)|\approx1$, within a narrow bandwidth ($\Delta\omega/\Omega_s\sim0.1\%$). The calculation with other losses, $1\times10^{-5}<\Gamma/\Omega_s<1\times10^{-1}$, provides similar results to Fig. 4.

In order to reduce losses in the scattered wave and to increase the bandwidth of the negative refractive index effect, we have considered additional doping with an *acceptor* (e.g., Cd of group II, or Ag of group I). If the acceptor has almost the same density as the density of Cr ($N_A\approx N_{\mathrm{Cr}}$), the effective total density of the electrons in the conduction band can be considerably reduced without affecting the permeability function, which depends only on $N_{\mathrm{Cr}}$. The plasmon frequency, $\omega_p$, will be much closer to the spin-wave frequency, $\Omega_s$, and, consequently, the region of overlapping of spin-wave resonance with plasmon resonance is much wider. If $\omega_p$ is smaller than $\Omega_s$ (or $n_e\leq3.5\times10^{17}$ cm$^{-3}$), the negative refractive index band disappears. Moreover, the losses in the plasmon subsystem increase above $n_e=4\times10^{17}$ cm$^{-3}$. Our calculations show that there is a characteristic plasmon frequency, $\omega_p=\omega_{\mathrm{Cr}}\sim10.8$ THz, which corresponds to $n_e=n_{\mathrm{Cr}}=3.5\times10^{17}$ cm$^{-3}$ where the losses from the plasmon subsystem are minimized and the resulting negative refractive index band has lower losses.

For this situation of additional doping with an acceptor, the results of the calculations, for $x=1.0$, with the moderate ($\Gamma/\Omega_s\approx1\times10^{-3}$) and high ($\Gamma/\Omega_s\approx1\times10^{-1}$) losses in the spin-wave subsystem are shown in Figs. 5 and 6, respectively. One can see a strongly pronounced negative refractive index band with a low loss ratio $\xi=|\mathrm{Im}(n)/\mathrm{Re}(n)|<0.45$ even for the highest possible losses in the magnetic subsystem ($\Gamma/\Omega_s\approx1\times10^{-1}$), as shown in Fig. 6. In the situation

of moderate losses in the magnetic subsystem ($\Gamma/\Omega_s \approx 1 \times 10^{-3}$), the loss ratio, $\xi \approx 0.4$, is also small.

Next, we have looked at the impact when the density of Cr decreases from $N_{\mathrm{Cr}} \approx 1.6 \times 10^{22} (1/\mathrm{cm}^3)$ ($x=1.0$) to $N_{\mathrm{Cr}} \approx 1 \times 10^{21}$ $(1/\mathrm{cm}^3)$ ($x=0.06$), keeping all other parameters the same as in Fig. 5. The appropriate results are shown in Fig. 7. As follows from these figures, the negative refractive index effect still survives with a moderate loss ratio $\xi \approx 0.6$.

In summary, the negative refractive index effect exists in all modeled situations, and the NIM band is stable with respect to change in the main design parameter, Cr dopant level, $x$, which is to be larger than $\sim 0.04$. Also, the effect was found to be stable with respect to the losses in the magnetic subsystem ($1 \times 10^{-5} < \Gamma/\Omega_s < 0.1$) and exists even for the worst case scenario of highest possible losses, $\Gamma/\Omega_s \sim 0.1$, when additional acceptor doping is considered. Also, one can see that the losses, $\xi \approx 0.4$, within the negative refractive index band are close to the total losses in the electric and magnetic subsystems. In the situation of inhomogeneous NIM designs,[8–19] the additional inhomogeneity-driven losses are normally an order of magnitude larger than losses in plasmonic subsystem.

Interestingly, the calculations show that the losses in the spin-wave subsystem, $\Gamma$, affect the negative refractive index effect much less dramatically than the losses, $\gamma$, in the plasmon subsystem. Nevertheless, despite the fact that the typical losses in the spin-wave subsystem ($1 \times 10^{-5} < \Gamma/\Omega_s \leq 1 \times 10^{-1}$) are smaller than the typical losses in plasmon subsystem $\gamma/\omega_p \sim 0.1$, the magnitude of $\Gamma$ is still an important factor for the negative refractive index effect. Since the experimentally measured typical bandwidth of the magnetic resonance in semiconductors constitutes 1–100 Oe,[45,46] the appropriate $\Gamma \sim (1 \times 10^7 - 1 \times 10^9)$ Hz corresponds to small dimensionless losses, $\Gamma/\Omega_s \sim 1 \times 10^{-6} - 1 \times 10^{-4}$. Also, the aforementioned loss level, $\Gamma \sim 1/\tau$, correlates well with both the calculation of the spin-wave relaxation time, $\tau \approx 1 \times 10^{-8}$ s, due to the magnon-phonon interactions[48] and experimental relaxation measurements, $\tau \approx (1 \times 10^{-6} - 1 \times 10^{-7})$ s, in ferromagnetic resonance.[47] As we have already mentioned above, in accordance with both the theoretical calculations and experimental results,[49,50] the losses become much larger (up to $\Gamma/\Omega_s \sim 1 \times 10^{-1}$) in the situation of the resonance when the wave vector of the spin wave belongs to Brillouin zone. It is important to stress that as follows from our calculations, the losses in the magnetic subsystem do not destroy the negative refractive index band, and the bottleneck of the effect is still the plasmonic subsystem.

## VI. CONCLUSIONS

In conclusion, based on the presented calculations, we predict that the homogeneous magnetic semiconductor $In_{2-x}Cr_xO_3$, in its polycrystalline form, should possess the negative refractive index effect at $\sim 10.48$ THz. The estimates of the reasonably narrow negative refractive index bandwidth $\Delta\omega/\Omega_s \sim 0.1\%$ along with the magnitude of the negative refractive index [$\mathrm{Re}(n) \sim -1.0$] and a decent loss ratio $|\mathrm{Im}(n)/\mathrm{Re}(n)| \leq 0.4$ support the viability of the suggested effect. The mechanism of the negative refractive index effect is due to the simultaneous considerable permittivity and permeability responses in the vicinity of the ferromagnetic resonance close to the boundary of the Brillouin zone. The dopant magnetic-moment-carrying atoms of Cr donate the electrons into the conduction band, and the indirect exchange interaction or Liu mechanism between the magnetic ions and the conduction electrons is responsible for the ferromagnetic behavior. In this situation, the equilibrium magnetization $M_0$, which enters the expression for the permeability function $\mu(\omega)$, increases with ratio $x$ of the Cr dopant. Since the permittivity function $\varepsilon(\omega)$ depends on the same parameter $x$ due to the donation of electrons into the conduction band (plasmon density), $x$ is an adjustable parameter of the theory. In our situation of $In_{2-x}Cr_xO_3$, the appropriate $x \sim (0.3-1.0)$ corresponds to heavy doping with Cr when every second In atom is substituted by Cr. We should mention that even much smaller $x \sim 0.1$ provides the ferromagnetic behavior of $In_{2-x}Cr_xO_3$ with Curie temperature well above room temperature, as we know from the experiment.[26] In accordance with our calculations, the negative refractive index effect should exist even in this situation although with more narrow band $\Delta\omega/\Omega_s < 0.01\%$ and high losses.

Since the homogeneous NIM designs obviously have several advantages over the traditional inhomogeneous metamaterials (i.e., easy of fabrication), we hope that the utilization of the magnetic semiconductors will be useful in fast-developing field of negative refractive index effect.

## ACKNOWLEDGMENT

This work was supported by a grant from NSF (Grant No. ECCS-0702467).

[1] L. I. Mandel'shtam, Zh. Eksp. Teor. Fiz. **15**, 475 (1945).
[2] H. Lamb, Proc. London Math. Soc. **s2-1**, 473 (1904).
[3] A. Schuster, *An Introduction to the Theory of Optics* (Edward Arnold, London, 1904).
[4] V. G. Veselago, Sov. Phys. Usp. **10**, 509 (1968).
[5] M. W. McCall, A. Lakhtakia, and W. S. Weiglhofer, Eur. J. Phys. **23**, 353 (2002).
[6] D. R. Smith, S. Schultz, P. Markos, and C. M. Soukoulis, Phys. Rev. B **65**, 195104 (2002).
[7] J. B. Pendry, Phys. Rev. Lett. **85**, 3966 (2000).
[8] J. B. Pendry, A. J. Holden, D. J. Robbins, and W. J. Stewart, IEEE Trans. Microwave Theory Tech. **47**, 2075 (1999).
[9] T. J. Yen, W. J. Padilla, N. Fang, D. C. Vier, D. R. Smith, J. B. Pendry, D. N. Basov, and X. Zhang, Science **303**, 1494 (2004).

[10] Shuang Zhang, Wenjun Fan, K. J. Malloy, S. R. J. Brueck, N. C. Panoiu, and R. M. Osgood, Opt. Express **13**, 4922 (2005).
[11] T. F. Gundogdu, N. Katsarakis, M. Kafesaki, R. S. Penciu, G. Konstantinidis, A. Kostopoulos, E. N. Economoy, and C. M. Soukoulis, Opt. Express **16**, 9173 (2008).
[12] Shuang Zhang, Wenjun Fan, Kevin J. Malloy, Steven R. J. Brueck, Nicolae C. Panoiu, and Richard M. Osgood, J. Opt. Soc. Am. B **23**, 434 (2006).
[13] Alexander V. Kildishev, Wenshan Cai, Uday K. Chettiar, Hsiao-Kuan Yuan, Andrey K. Sarychev, Vladimir P. Drachev, and Vladimir M. Shalaev, J. Opt. Soc. Am. B **23**, 423 (2006).
[14] Nader Engheta and R. W. Ziolkowski, IEEE Trans. Microwave Theory Tech. **53**, 1535 (2005).
[15] A. N. Grigorenko, A. K. Geim, H. F. Gleeson, Y. Zhang, A. A. Firsov, I. Y. Khrushchev, and J. Petrovic, Nature (London) **438**, 335 (2005).
[16] Gunnar Dolling, Christian Enkrich, Martin Wegener, Costas M. Soukoulis, and Stefan Linden, Science **312**, 892 (2006).
[17] Adil-Gerai Kussow, Alkim Akyurtlu, Andrey Semichaevsky, and Niwat Angkawisittpan, Phys. Rev. B **76**, 195123 (2007).
[18] G. Dolling, M. Wegener, C. M. Soukoulis, and S. Linden, Opt. Lett. **32**, 53 (2007).
[19] T. Koschny, L. Zhang, and C. M. Soukoulis, Phys. Rev. B **71**, 121103(R) (2005).
[20] E. M. Lifshitz, L. D. Landau, and L. P. Pitaevskii, *Electrodynamics of Continuous Media*, Course of Theoretical Physics Vol. 8, 2nd ed. (Pergamon, London, 1984), p. 210.
[21] J. Kastel, M. Fleischhauer, S. F. Yelin, and R. L. Walsworth, Phys. Rev. Lett. **99**, 073602 (2007).
[22] Q. Thommen and P. Mandel, Phys. Rev. Lett. **96**, 053601 (2006).
[23] M. O. Oktel and O. E. Mustecaplioglu, Phys. Rev. A **70**, 053806 (2004).
[24] E. L. Nagaev, *Physics of Magnetic Semiconductors* (MIR, Moscow, 1983).
[25] K. L. Chopra, S. Major, and D. K. Pandya, Thin Solid Films **102**, 1 (1983).
[26] Scott S. Layne (http://www.hwscience.com/HWJS/archives/CIO/CIO.html).
[27] A. I. Akhiezer, V. G. Bar'yakhtar, and S. V. Peletminskii, *Spin Waves* (Wiley, New York, 1968), p. 54.
[28] A. Pimenov, A. Loidl, K. Gehrke, V. Moshnyaga, and K. Samwer, Phys. Rev. Lett. **98**, 197401 (2007).
[29] R. H. Tarkhanyan and D. G. Niarchos, J. Magn. Magn. Mater. **312**, 6 (2007).
[30] Yong Zhang, B. Fluegel, and A. Mascarenhas, Phys. Rev. Lett. **91**, 157404 (2003).
[31] A. J. Hoffman, L. Alekseev, S. S. Howard, K. J. Franz, D. Wasserman, V. A. Podolsky, E. E. Narimanov, D. L. Sivco, and C. Gmachl, Nature Mater. **6**, 946 (2007).
[32] T. G. Mackay and A. Lakhtakia, Microwave Opt. Technol. Lett. **49**, 874 (2007).
[33] M. T. Johnson and E. G. Visser, IEEE Trans. Magn. **26**, 1987 (1990).
[34] L. Daniel and R. Corcolle, IEEE Trans. Magn. **43**, 3153 (2007).
[35] S. H. Liu, Phys. Rev. **121**, 451 (1961).
[36] A. Anselm, *Introduction to Semiconductor Theory* (MIR, Moscow, 1981).
[37] J. Szczyrbowski, A. Dietrich, and H. Hoffmann, Phys. Status Solidi A **69**, 217 (1982).
[38] S. Zh. Karazhanov, P. Ravindran, P. Vajeeston, A. Ulyashin, T. G. Finstad, and H. Fjellvag, Phys. Rev. B **76**, 075129 (2007).
[39] J. Friedel, *Dislocations* (Pergamon, Oxford, 1964), p. 282.
[40] J. P. Hirth and J. Lothe, *Theory of Dislocations* (McGraw-Hill, New York, 1968), p. 644.
[41] J. E. Medvedeva, Appl. Phys. A: Mater. Sci. Process. **89**, 43 (2007).
[42] math.fullerton.edu/mathews/n2003/MonteCarloMod.html
[43] *Handbook of Optical Constants of Solids*, edited by E. D. Palik, G. Ghosh, and B. Jenses (Academic, New York, 1998), Vol. II, p. 126.
[44] H. L. Hartnagel, A. L. Dawar, A. K. Jain, and C. Jagadish, *Semiconducting Transparent Thin Films* (Institute of Physics, Bristol, 1995).
[45] C. Kittel, Phys. Rev. **110**, 836 (1958).
[46] E. Schlomann, Phys. Rev. **121**, 1312 (1961).
[47] N. Bloembergen and S. Wang, Phys. Rev. **93**, 72 (1954).
[48] C. Kittel, Phys. Rev. **110**, 1295 (1958).
[49] K. N. Trohidou, J. A. Blackman, and J. F. Cooke, Phys. Rev. Lett. **67**, 2561 (1991).
[50] J. W. Lynn, Phys. Rev. B **11**, 2624 (1975).